



Population genetics of swamp eel in the Yangtze River: comparative analyses between mitochondrial and microsatellite data provide novel insights

Huaxing Zhou*, Yuting Hu*, He Jiang, Guoqing Duan, Jun Ling, Tingshuang Pan, Xiaolei Chen, Huan Wang and Ye Zhang

Anhui Key Laboratory of Aquaculture and Stock Enhancement, Fisheries Research Institution, Anhui Academy of Agricultural Sciences, Hefei, China

*These authors contributed equally to this work.

ABSTRACT

The swamp eel (*Monopterus albus*) is a typical sex reversal fish with high economic value. Several phylogeographic studies have been performed using various markers but comparative research between mitochondrial and nuclear markers is rare. Here, a fine-scale study was performed across six sites along the Yangtze River including three sites on the main stem and three sites from tributaries. A total of 180 swamp eel individuals were collected. Genetic structure and demographic history were explored using data from two mitochondrial genes and eight microsatellite loci. The results revealed the samples from tributary sites formed three separate clades which contained site-specific lineages. Geographic isolation and the habitat patchiness caused by seasonal cutoff were inferred to be the reasons for this differentiation. Strong gene flow was detected among the sites along the main stem. Rapid flow of the river main stem may provide the dynamic for the migration of swamp eel. Interestingly, the comparative analyses between the two marker types was discordant. Mitochondrial results suggested samples from three tributary sites were highly differentiated. However, microsatellite analyses indicated the tributary samples were moderately differentiated. We conclude this discordance is mainly caused by the unique life history of sex reversal fish. Our study provides novel insights regarding the population genetics of sex reversal fish.

Submitted 31 July 2019
Accepted 16 December 2019
Published 21 January 2020

Corresponding author
He Jiang, kenc7c7c7@126.com

Academic editor
Lee Rollins

Additional Information and
Declarations can be found on
page 11

DOI 10.7717/peerj.8415

© Copyright
2020 Zhou et al.

Distributed under
Creative Commons CC-BY 4.0

Subjects Aquaculture, Fisheries and Fish Science, Biogeography, Genetics, Molecular Biology, Population Biology

Keywords *Monopterus albus*, Sex reversal, Mitochondrial and nuclear markers, Population genetics

INTRODUCTION

The swamp eel (*Monopterus albus*) is a typical sex reversal fish, belonging to the family Synbranchidae, which usually inhabits swamps, ponds and rice fields (Nelson, Grande & Wilson, 2016). Due to its high nutritional value and good taste, the swamp eel is used as a significant aquatic food in China. In 2018, 0.32 million tons of swamp eel were produced by Chinese aquaculture (data from The Ministry of Agriculture of China, 2019).

OPEN ACCESS

With the development of swamp eel farming, population genetic research of the wild eel became a hot topic, which has been used to guide the genetic breeding and swamp eel aquaculture. Several studies have used different markers including microsatellites, mitochondrial sequences and Inter-Simple Sequence Repeats (ISSR) to explore swamp eel population genetics (Lei et al., 2012; Li et al., 2013; Liang et al., 2016). Previous studies suggested a rapid decrease of wild swamp eel caused by the large use of pesticides and over-exploitation (Li et al., 2013; Liang et al., 2016). Cultured populations were genetically less diverse than wild populations. Due to farm escapes, the populations of wild swamp eel suffer from genetic homogenization and degeneration of genetic characters (Li et al., 2013). Thus, further research of population genetics and dynamics are necessary to protect the wild swamp eel.

Monopterus albus is a sex reversal fish with a unique life history (Liu, 1944; Mazzoni et al., 2018; Qu, 2018). It starts the reproductive cycle as a functional female. During 1 to 1.5 years of age, females obtain well-developed ova. After spawning, the swamp eel's sex is reversed from female to male. The intersexes appear in the two-year-old age class. Then it lives as male without sex reversal (Liem, 1963). Generally, swamp eels can live to 6-8 years. Mitochondrial DNA is maternally inherited. For this reason, the inheritance patterns of protogynous hermaphrodites differ to that of species that do not practice sex reversal (Coscia et al., 2016). Therefore, it may be important to include both nuclear and mitochondrial markers to explore the population genetics of sex reversal fish.

This fine-scale study was performed across six sites along the Yangtze River including three sites on the main stem and three sites from tributaries. Subsequently, the genetic structure of these six sampling sites was explored, using sequence from two mitochondrial genes and eight microsatellite loci. Here, we show how different types of molecular markers can provide new insights regarding the population genetics of sex reversal fish.

MATERIALS & METHODS

Ethics statement and Sample collection

Procedures involving animals and their care were approved by the Animal Care and Use Committee of Anhui Academy of Agricultural Sciences under approval number 201003076. Field experiments were approved by Fisheries Bureau of Anhui (project number: FB/AH 2017-10).

A total of 180 individuals were collected using net from six sites along the Anhui basin of the Yangtze River (Table S1). Sampling sites from tributaries of the Yangtze River included Dang Tu (DT), Fan Chang (FC) and Huai Ning (HN); sampling sites from the main stem of the Yangtze River included Wu Wei (WW), Gui Chi (GC) and Wang Jiang (WJ) (Fig. 1).

DNA extraction and Marker genotyping

Total genomic DNA was extracted from muscle tissue using a standard phenol/chloroform procedure via proteinase K digestion (Sambrook, Fritsch & Maniatis, 1989), and then kept at -20°C for PCR amplification.

The mitochondrial cytochrome c oxidase subunit I (COI) gene and cytochrome b (Cyt b) gene were chosen. Two pairs of primers were designed here for the amplification (Table

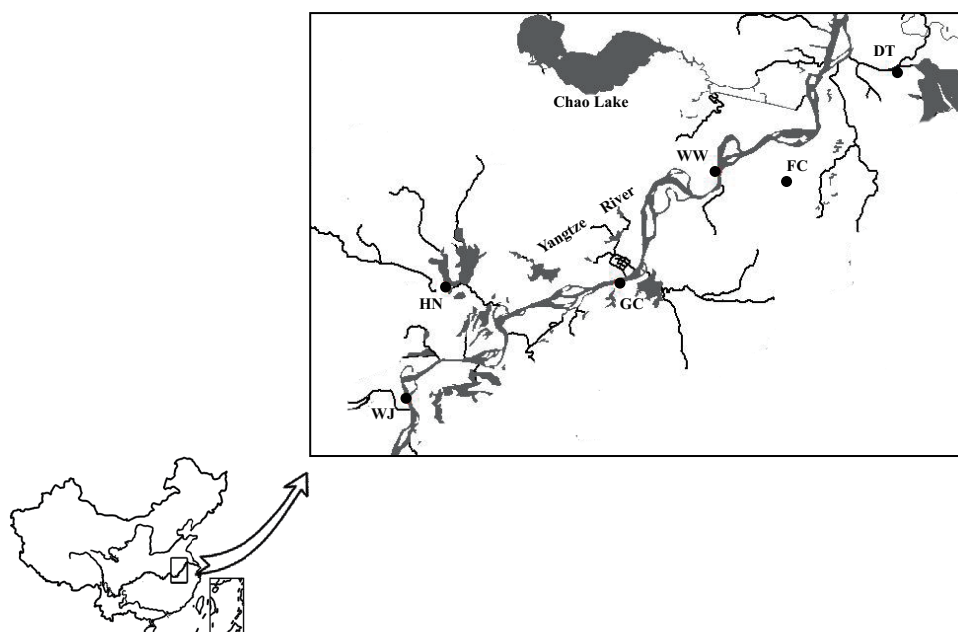


Figure 1 Sampling sites along the Yangtze River mapped using DIVA-GIS. Three sampling sites from main stem included Wu Wei (WW), Gui Chi (GC) and Wang Jiang (WJ); three sampling sites from tributaries included Dang Tu (DT), Fan Chang (FC) and Huai Ning (HN). FC tributary connected to the main stem during the wet season and isolated during the dry season. Data source: DIVA-GIS (<http://swww.diva-gis.org/Data>).

Full-size  DOI: [10.7717/peerj.8415/fig-1](https://doi.org/10.7717/peerj.8415/fig-1)

S2). PCR were conducted in 50 μ L reaction mixtures containing 200 ng template DNA, 5 μ L 10 \times buffer (TaKaRa, Dalian, China), 4 μ L MgCl₂ (2.5 mol/L), 3 μ L dNTP (2.5 mmol/L), 2 μ L of each primer (5 μ mol/L), and 1 U Taq DNA polymerase (5 U/ μ L, TaKaRa). PCR conditions were as follows: initial denaturation (95 $^{\circ}$ C, 1 min), then 35 cycles of denaturation (94 $^{\circ}$ C, 50 s), primer annealing (55 $^{\circ}$ C, 45 s), and elongation (72 $^{\circ}$ C, 1 min) and a final extension (72 $^{\circ}$ C, 10 min). All fragments were sequenced in both directions with an ABI3730 automated sequencer (Invitrogen Biotechnology Co., Ltd, USA). Then these two gene sequences were combined for subsequent analyses.

Eight unlinked polymorphic microsatellite loci were selected from previous studies (Table S1) (Lei et al., 2012; Li et al., 2007; Zhuo et al., 2011). PCR were conducted in 50 μ L reaction mixtures containing 200 ng template DNA, 5 μ L 10 \times buffer (TaKaRa, Dalian, China), 4 μ L MgCl₂ (2.5 mol/L), 2.5 μ L dNTP (2.5 mmol/L), 2 μ L of each primer (5 μ mol/L), and 1 U Taq DNA polymerase (25 U/ μ L, TaKaRa). PCR conditions were as follows: initial denaturation (95 $^{\circ}$ C, 5 min), then 32 cycles of denaturation (94 $^{\circ}$ C, 30 s), primer annealing (57 $^{\circ}$ C, 60 s), and elongation (72 $^{\circ}$ C, 90 s) and a final extension (72 $^{\circ}$ C, 5 min). Genotypes were detected by ABIPRISM 3730.

DATA ANALYSES

Mitochondrial sequence

Sequences were assembled by DNASTAR Lasergene package. Subsequent homologous alignment was performed by Mafft v.7 online program (<https://mafft.cbrc.jp/alignment/software/>) (Kato, Rozewicki & Yamada, 2019).

Haplotype and nucleotide diversity were estimated using DNAsp V.6 (Rozas et al., 2017). A haplotype network was constructed using Median Joining (MJ) in NETWORK v.5.0 (Bandelt, Forster & Röhl, 1999). Analysis of Molecular Variance (AMOVA) was performed using Arlequin v.3.11 (Excoffier, Laval & Schneider, 2005). Genetic variation within and among sampling sites was assessed. Pairwise F_{st} was estimated in order to evaluate the levels of population differentiation (Slatkin & Barton, 1989) and the P values were corrected using multiple testing.

The demographic history was explored using three approaches, e.g., neutrality tests, mismatch distribution and Bayesian Skyline Plots (BSP) analyses. Tajima's D (Tajima, 1989) and Fu's F_s (Fu, 1997) values were calculated using DNAsp V.6. Mismatch distribution analyses were performed using Arlequin v.3.11 (Rogers & Harpending, 1992). The expansion time was calculated by the τ value with the equation $\tau = 2 \mu t$, where μ represents the nucleotide mutation rate and t represents the estimated expansion time. BSP analysis was performed using Beast v1.10.4 (Suchard et al., 2018) under an uncorrelated relaxed clock mode for 5×10^7 generations.

Microsatellites data

The results of 8 microsatellites loci were read using GeneMarker (Holland & Parson, 2011) and reformatted using Convert v.1.31 (Glaubitz, 2004). Hardy-Weinberg equilibrium (HWE) tests were performed using Popgene v 1.32 (Yeh et al., 1997). Expected and observed heterozygosity were calculated with Arlequin v.3.11 (Rogers & Harpending, 1992). AMOVA was implemented with Arlequin. Pairwise F_{st} was computed based on Slatkin's method (Slatkin & Barton, 1989). The geographical and genetic distance between sample sites was measured by GPS and Popgene v 1.32, respectively. The correlation between geographical and genetic distance was analyzed using Pcord v 5 (Grandin, 2006).

Population structure was estimated using an MCMC (Markov Chain Monte Carlo) algorithm as implemented in Structure v.2.3.3 (Hubisz et al., 2009). The number of clusters (K) was calculated under 1×10^6 iterations with 10 replications and the optimal number of K was deduced by Structure Harvester Web v.0.6.94 (Evanno, Regnaut & Goudet, 2005; Earl, 2012).

RESULTS

Mitochondrial genes

A total of 1752 bp of mitochondrial sequence (COI 665 bp, Accession number: MN097948–MN098127; Cyt b 1087 bp, Accession number: MN098128–MN098307) were obtained for analyses. The contents of the bases A, T, G and C were 24.6%, 29.3%, 14.6% and 31.5% respectively, which showed obvious anti-G bias (Saccone et al., 1999).

Table 1 Genetic diversity of samples from six sites assessed using mitochondrial and microsatellite data.

Sampling sites	Mitochondrial genes			Microsatellite loci		
	Num. of haplotypes	<i>Hd</i>	<i>Pi</i>	Num. of alleles	<i>He</i>	<i>Ho</i>
DT (Tributary)	18	0.9540	0.0148	14	0.8749	0.7917
WW (Main stem)	24	0.9793	0.0078	14	0.8638	0.7292
FC (Tributary)	9	0.6620	0.0017	12	0.8089	0.6542
GC (Main stem)	15	0.8480	0.0021	13	0.8420	0.7417
HN (Tributary)	13	0.9220	0.0072	12	0.8052	0.5958
WJ (Main stem)	19	0.9240	0.0023	14	0.8516	0.7802

Notes. *Hd* represents haplotype diversity; *Pi* represents nucleotide diversity; *He* represents expected heterozygosity; *Ho* represents observed heterozygosity.

The 180 mitochondrial sequences corresponded to 86 distinct haplotypes (Table 1). All haplotypes were divided into four clades based on MJ method (Fig. 2). Clade A was the largest one which contained samples from five sampling sites. Haplotype 5 (H-5) had the largest number of shared individuals, and its central placement in the network suggests that this is the ancestral haplotype. The other three clades were separated by 13, 47, 24 mutational steps, respectively. Clade B and C only contained samples from the HN and FC sampling sites, respectively. Clade D mainly consisted of DT samples.

Haplotype diversity ranged from 0.6620 to 0.9793 and nucleotide diversity ranged from 0.0017 to 0.0148 based on mitochondrial sequence (Table 1). The results of AMOVA showed that genetic variation among sampling sites (71.23%, $P < 0.001$) were much higher than the variation within the sampling sites (28.77%, $P < 0.001$) (Table 2A). Subsequent F_{st} values further confirmed this result. Strong gene flow was detected between the main stem sampling sites ($F_{st} = 0.0242$ between GC and WW, $F_{st} = 0.0286$ between WJ and WW, $F_{st} = 0.0305$ between WJ and GC, see Table 3A). And high differentiation was revealed between the tributary sampling sites ($F_{st} = 0.3069 - 0.9431$) (Table 3A). Fu's F_s and Tajima's D tests of main stem samples were significant ($P < 0.01$) but negative. No explicit expansion or decline were revealed for the tributary samples and the Fu's F_s and Tajima's D values except the Tajima's D of FC were not significant (Table 4). Mismatch distribution analysis revealed similar results. The values of sum of squares deviations (SSD) for samples from main stem and DT were not significant ($P > 0.05$), indicating that sudden expansion could not be rejected (Table 4). The BSP analysis suggested the main stem samples had expanded roughly in 0.46 MYA (Fig. 3).

Microsatellite loci

The eight microsatellite loci amplified unambiguous and repeatable products in the size range expected. All loci were in Hardy-Weinberg equilibrium ($P > 0.05$). High genetic diversity was also supported by microsatellite data. Expected and observed heterozygosity for the six sampling sites were 0.8052–0.8749 and 0.5958–0.7917, respectively (Table 1).

Structure results suggested the highest posterior probability for $K = 4$ (Fig. S1). The ΔK method revealed four potential genetic clusters, aligning with the three tributaries and

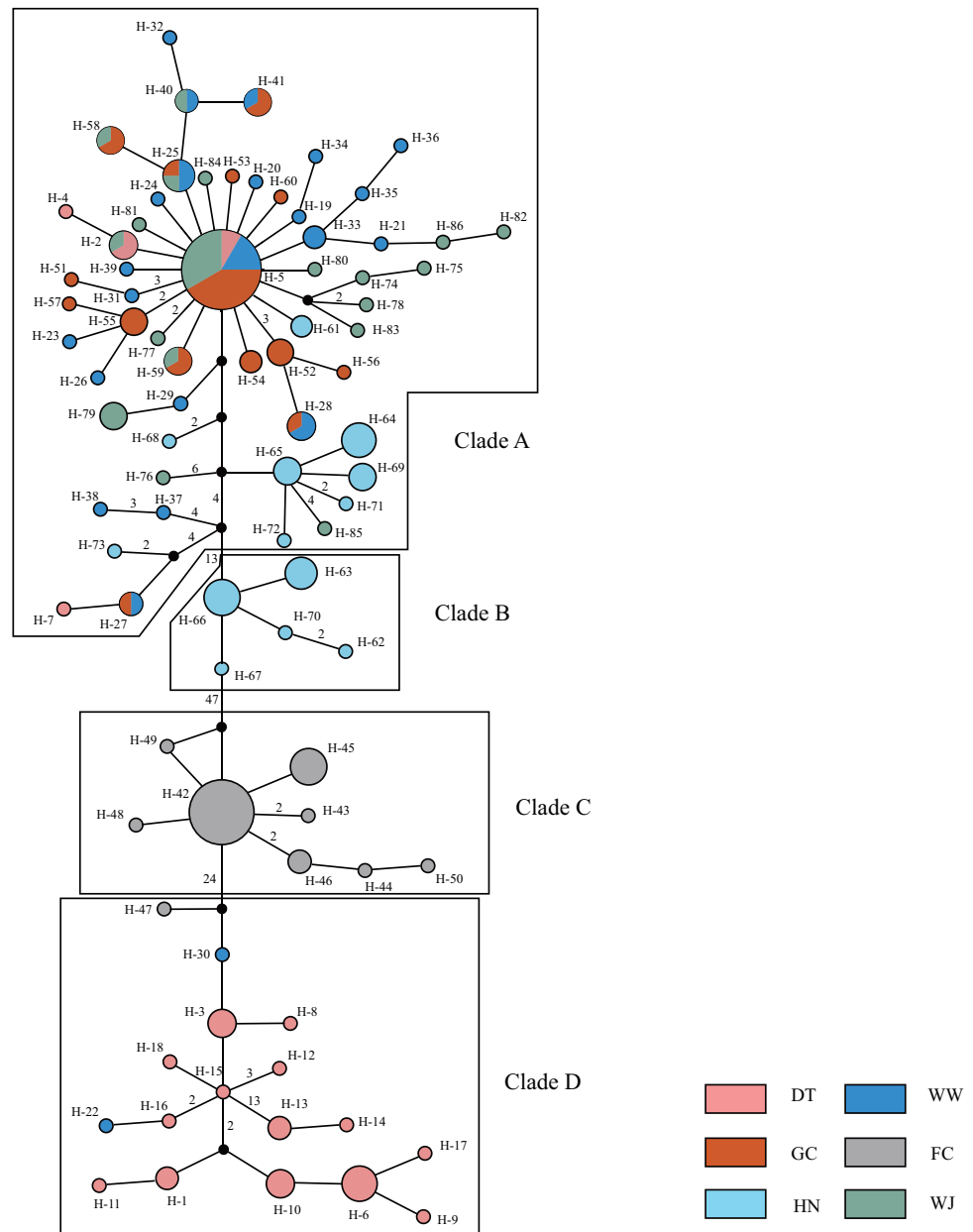


Figure 2 Haplotype network showing the genetic relationship of samples using Median Joining (MJ) method. Different colors represent the six populations. Circle size represents the number of sequence. The largest circle represents $n = 24$ and the smallest circle represent $n = 1$. Numbers of nearby branches represent the mutational steps and no numbers represent only one mutational step. Black dots represent Median Vector (mv).

Full-size [DOI: 10.7717/peerj.8415/fig-2](https://doi.org/10.7717/peerj.8415/fig-2)

all the main stem sites together. Samples from main stem showed high levels of genetic admixture (Fig. 4).

AMOVA was performed using the microsatellite data and suggested that genetic variation was mainly within sampling sites (94.65%, $P < 0.001$), opposite to the results

Table 2 AMOVA of 6 sampling sites indicating the source of variation.**Table 2a** AMOVA of 6 sampling sites indicating the source of variation by mitochondrial data used.

Source of variation	df	Sum of squares	Percentage of variation	P value
Among sampling sites	5	1965.433	71.23	<0.001
Within sampling sites	174	908.533	28.77	<0.001
Total	179	2873.967		

Table 2b AMOVA of 6 sampling sites indicating the source of variation by microsatellite loci used.

Source of variation	df	Sum of squares	Percentage of variation	P value
Among sampling sites	5	76.325	5.35	<0.001
Within sampling sites	352	672.105	94.65	<0.001
total	357	1260.43		

Table 3 Pairwise values of F_{st} (below diagonal) and P (above diagonal) between sampling sites.**Table 3a** Pairwise values of F_{st} (below diagonal) and P (above diagonal) between sampling sites estimated using mitochondrial data.

	DT	WW	FC	GC	HN	WJ
DT		<0.01	<0.01	<0.01	<0.01	<0.01
WW	0.6228		<0.01	0.08	<0.01	0.05
FC	0.5800	0.8510		<0.01	<0.01	<0.01
GC	0.7296	0.0242	0.9431		<0.01	<0.01
HN	0.6441	0.3069	0.8551	0.4750		<0.01
WJ	0.7253	0.0286	0.9391	0.0305	0.4594	

Table 3b Pairwise values of F_{st} (below diagonal) and P (above diagonal) between sampling sites estimated using microsatellite loci.

	DT	WW	FC	GC	HN	WJ
DT		<0.01	<0.01	<0.01	<0.01	<0.01
WW	0.0653		<0.01	0.06	<0.01	0.37
FC	0.0813	0.0509		<0.01	<0.01	<0.01
GC	0.0794	0.0077	0.0585		<0.01	0.63
HN	0.0982	0.0597	0.0869	0.0636		<0.01
WJ	0.0704	0.0030	0.0509	0.0005	0.0493	

Table 4 Summary of neutrality and mismatch analyses indicating the demographic history.

Populations	Tajima's D	Fu's F_s	τ	SSD (P)
Main stem	-2.3328**	-24.9078**	2.2949	0.0056(0.36)
DT	0.6878	1.8735	0.3906	0.0344(0.53)
FC	-2.4163**	-0.8094	0.375	0.1446(0.02)
HN	0.4788	2.1653	22.5293	0.0496(0.008)

Notes.

** $P < 0.01$.

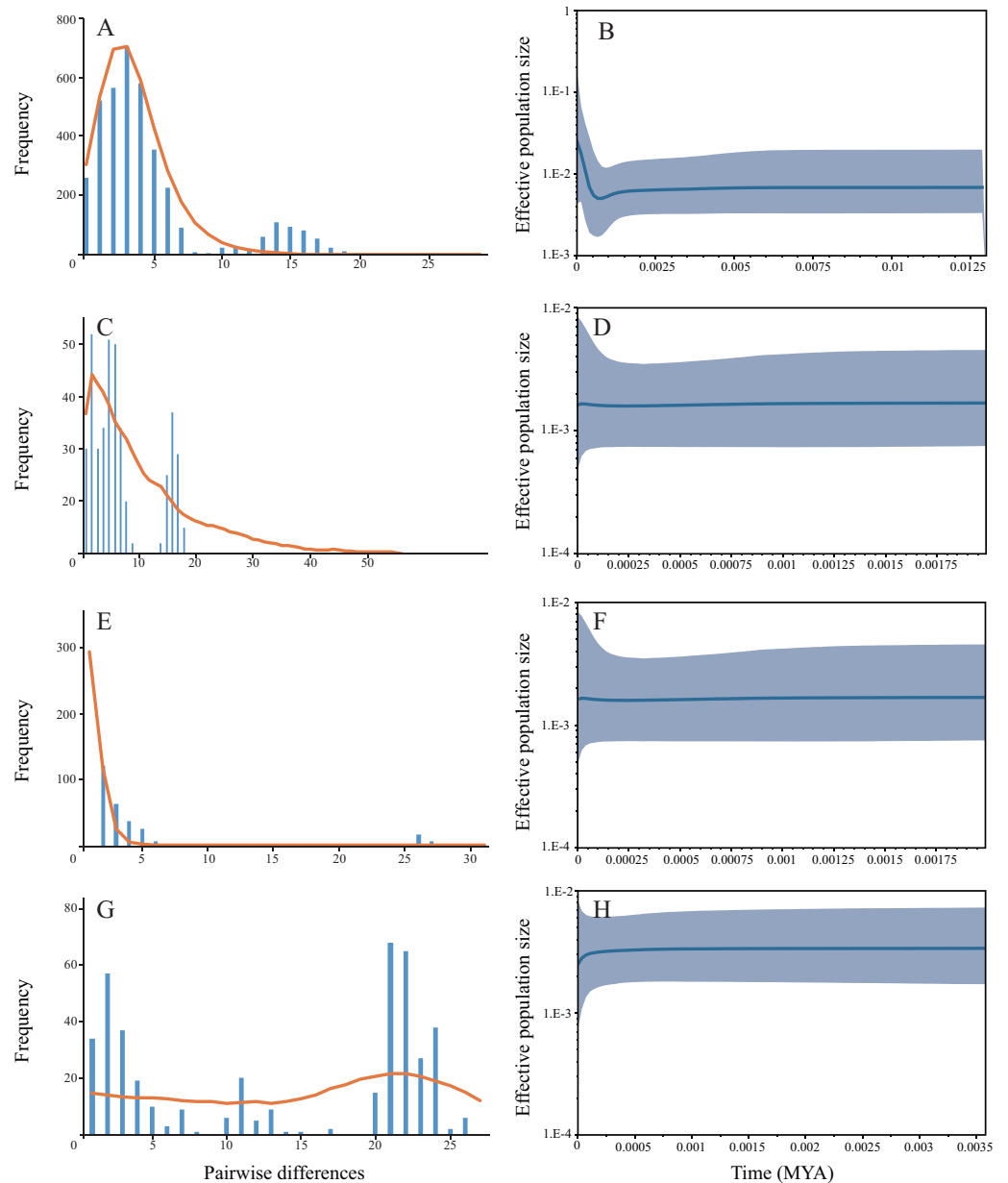


Figure 3 The demographic history inferred from mitochondrial data. Samples from three main stem sampling sites were treat as one group. (A) Mismatch distribution of main stem samples; (B) Bayesian skyline plots of main stem samples, the shaded area represents the 95% confidence intervals of Highest Posterior Density (HPD) analysis; (C) Mismatch distribution of DT samples; (D) Bayesian skyline plots of DT samples; (E) Mismatch distribution of FC samples; (F) Bayesian skyline plots of FC samples; (G) Mismatch distribution of HN samples; (H) Bayesian skyline plots of HN samples.

Full-size  DOI: [10.7717/peerj.8415/fig-3](https://doi.org/10.7717/peerj.8415/fig-3)

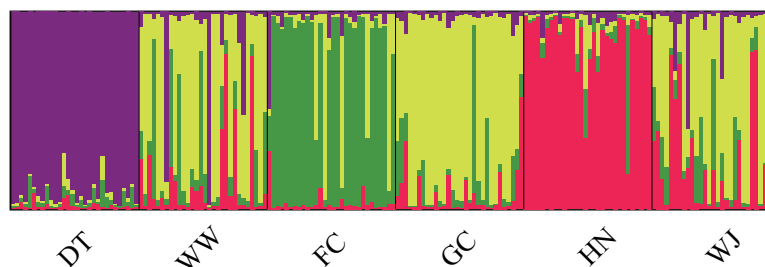


Figure 4 Population structure of 180 swamp eels showing for $K = 4$. Four colors, e.g., red, yellow, purple and green, represent the inferred genetic clusters.

Full-size  DOI: 10.7717/peerj.8415/fig-4

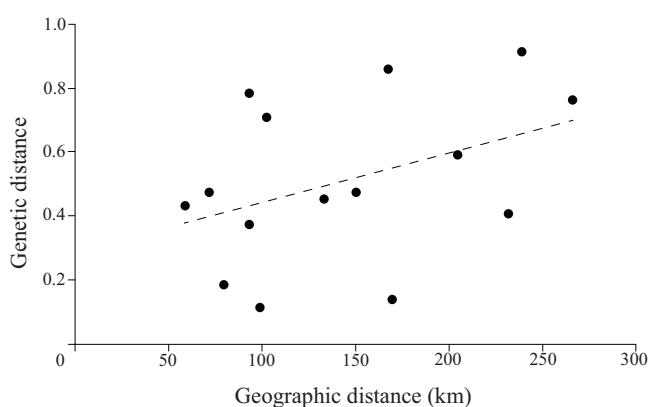


Figure 5 Plotmatrix indicating the correlation between genetic and geographic matrices.

Full-size  DOI: 10.7717/peerj.8415/fig-5

from mitochondrial data (Table 2B). F_{st} values suggested low levels of differentiation ($F_{st} = 0.0005 - 0.0982$) (Table 3B).

The correlation between genetic and geographic matrixes was assessed using Mantel test (Table S3). The results suggested a significant correlation between them ($r = 0.8791$, $P = 0.004$) (Fig. 5).

DISCUSSION

Population genetics of swamp eel

High levels of genetic diversity were found across sampling sites at both mitochondrial and microsatellite markers. The genetic diversity level of this study except FC sample site was higher than previous study in the same basin ($Hd = 0.708$ and $Pi = 0.002$ based on mitochondrial D-loop sequences) (Liang et al., 2016). The genetic diversity of FC samples was the lowest ($Hd = 0.6620$, $Pi = 0.0017$). The significant differentiation of three tributary sampling sites was revealed by the population genetic analyses ($F_{st} > 0.25$). The haplotype network and structure results suggested the tributary samples formed three separate clades which contained site-specific lineages. Significant correlation between genetic and

geographic distance was detected. Interestingly, strong gene flow was detected among the main stem sampling sites and the expansion of main stem samples was detected.

It is well known that the swamp eel is a burrowing fish whose fins are vestigial or absent (Nelson, Grande & Wilson, 2016). Compared with most fishes, the swimming ability of eel is weak. Thus, we were curious about the reasons for this long-distance gene flow among main stem sampling sites. The flow rate of main stem in Anhui basin range up to 1.0 m/s (Guo & Xia, 2007). Rapid flow provides the dynamic for the migration of swamp eel. The eggs and juvenile fishes can slip downstream to the farther places. However, due to the flat stream gradient and curved channel, the tributary flow becomes slower (Zhang, YT & Jiang, 2008) and long-distance migration is difficult for swamp eel. We propose that geographic isolation and the habitat patchiness caused by seasonal cutoff are the reasons for the differentiation between tributary samples. The tributary of FC site was much more isolated from the main stem. It connected to the main stem during the wet season and isolated during the dry season. Long-term isolation from the main stem may cause the low genetic diversity of FC samples.

Comparative analyses between mitochondrial and microsatellite data

Analyses of nuclear and mitochondrial markers revealed discordant population structure. Based on mitochondrial data, genetic variation was mainly found among sampling sites. Samples between the tributary sites were highly differentiated ($F_{st} > 0.25$) and represented three monophyletic clades. However, microsatellite analyses suggest that the majority of genetic variation is within these sampling sites; samples between the tributary sites were moderately differentiated ($0.05 < F_{st} < 0.15$). Mean F_{st} values among six sampling sites based on mitochondrial and microsatellite data were 0.548 and 0.055, respectively. The mean mitochondrial F_{st} value (0.548) was almost ten times higher than the F_{st} (0.055) estimated with microsatellite data.

Our study provided an interesting pattern of discordance between markers for population genetics. According to previous studies, sex-biased dispersal, genetic admixture and lineage sorting may be the potential reasons for the discordance caused by different molecular markers (Funk & Omland, 2003; Qu et al., 2012; Yang et al., 2016; Zarza, Reynoso & Emerson, 2011). Considering the sex reversal in this species, we inferred the unique life history of the swamp eel contributed to this discordance. Initially, the swamp eel is female and provides both mitochondrial and nuclear DNA to the population genetic pool. After spawning, the swamp eel becomes male. Male swamp eels are much bigger and stronger than females. Males could migrate farther and have a higher survival rates, which provides a potential of male sex-biased dispersal. Due to mitochondrial maternal inheritance, male swamp eels only provide nuclear DNA to the population genetic pool (Fig. 6). So male sex-biased dispersal may cause the differences in population structure between the markers. As mentioned above, male stage is much longer than female stage in the whole life of swamp eel that may cause different genetic frequencies between mitochondrial and nuclear data. The ten-fold difference between mitochondrial and nuclear F_{st} values also confirmed this hypothesis.

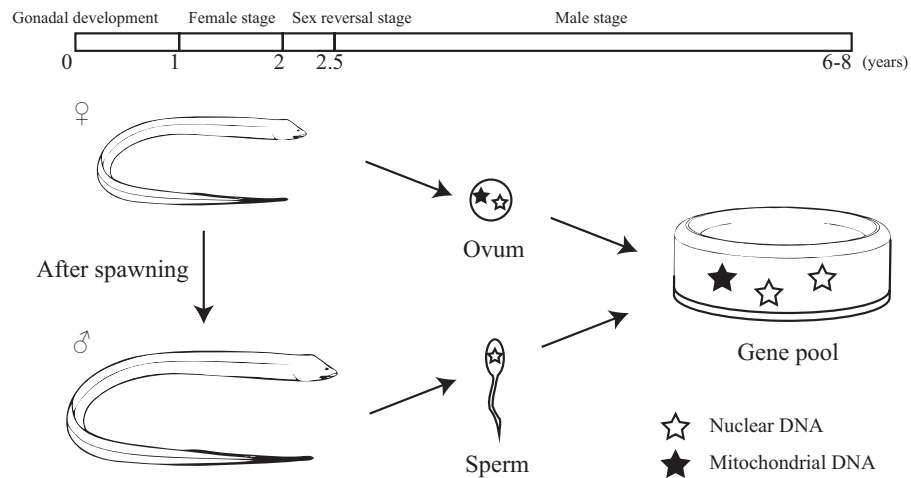


Figure 6 Diagram showing the unique life history and different hereditary patterns of mitochondrial DNA and nuclear DNA in sex reversal fish.

Full-size DOI: [10.7717/peerj.8415/fig-6](https://doi.org/10.7717/peerj.8415/fig-6)

CONCLUSIONS

Our study used two data sets, mitochondrial DNA and microsatellites, to explore the demography, genetic variation and population structure of swamp eels. Compared with previous studies, high levels of genetic diversity suggest that swamp eels are an abundant resource in the Anhui basin and have potential commercial value. Samples from each tributary site in this study should be treated as an independent genetic unit. The unique sex reversal life history of the swamp eel may be a significant factor affecting the population genetic structure and may generate the discordance we found between different molecular markers. Our study provides novel insights regarding the population genetics of sex reversal fish.

ACKNOWLEDGEMENTS

We thank Assoc. Prof. Lee Rollins, Adomas Ragauskas, Joana Robalo and Dr. Yangyang Liang for their constructive comments.

ADDITIONAL INFORMATION AND DECLARATIONS

Funding

This work was funded by the Earmarked Fund of Anhui Fishery Research System (No. 2016-84), Anhui Academy of Agricultural Sciences Technology Innovation Team (No. 2019YL026) and Chinese agriculture research system (No. CARS-48). The funders had no role in study design, data collection and analysis, decision to publish, or preparation of the manuscript.

Grant Disclosures

The following grant information was disclosed by the authors:

Earmarked Fund of Anhui Fishery Research System: No. 2016-84.

Anhui Academy of Agricultural Sciences Technology Innovation Team: No. 2019YL026.

Chinese agriculture research system: No. CARS-48.

Competing Interests

The authors declare there are no competing interests.

Author Contributions

- Huaxing Zhou conceived and designed the experiments, analyzed the data, prepared figures and/or tables, authored or reviewed drafts of the paper, and approved the final draft.
- Yuting Hu conceived and designed the experiments, performed the experiments, authored or reviewed drafts of the paper, and approved the final draft.
- He Jiang conceived and designed the experiments, authored or reviewed drafts of the paper, and approved the final draft.
- Guoqing Duan analyzed the data, authored or reviewed drafts of the paper, and approved the final draft.
- Jun Ling performed the experiments, authored or reviewed drafts of the paper, and approved the final draft.
- Tingshuang Pan, Xiaolei Chen performed the experiments, prepared figures and/or tables, and approved the final draft.
- Huan Wang and Ye Zhang analyzed the data, prepared figures and/or tables, authored or reviewed drafts of the paper, and approved the final draft.

Animal Ethics

The following information was supplied relating to ethical approvals (i.e., approving body and any reference numbers):

Procedures involving animals and their care were approved by the Animal Care and Use Committee of Anhui Academy of Agricultural Sciences under approval number 201003076.

Field Study Permissions

The following information was supplied relating to field study approvals (i.e., approving body and any reference numbers):

Field experiments were approved by Fisheries Bureau of Anhui (project number: FB/AH 2017-10).

Data Availability

The following information was supplied regarding data availability:

The mitochondrial *COI* and *Cyt b* genes are available at GenBank: [MN097948–MN098127](#) and [MN098128–MN098307](#). Additional data is available in the [Supplemental Files](#).

Supplemental Information

Supplemental information for this article can be found online at <http://dx.doi.org/10.7717/peerj.8415#supplemental-information>.

REFERENCES

- Bandelt HJ, Forster P, Röhl A. 1999.** Median-joining networks for inferring intraspecific phylogenies. *Molecular Biology and Evolution* **16**:37–48
DOI [10.1093/oxfordjournals.molbev.a026036](https://doi.org/10.1093/oxfordjournals.molbev.a026036).
- Coscia I, Chopelet J, Waples RS, Mann BQ, Marian S. 2016.** Sex change and effective population size: implications for population genetic studies in marine fish. *Heredity* **117**:251 DOI [10.1038/hdy.2016.50](https://doi.org/10.1038/hdy.2016.50).
- Earl DA. 2012.** STRUCTURE HARVESTER: a website and program for visualizing STRUCTURE output and implementing the Evanno method. *Conservation Genetics Resources* **4**:359–361 DOI [10.1007/s12686-011-9548-7](https://doi.org/10.1007/s12686-011-9548-7).
- Evanno G, Regnaut S, Goudet J. 2005.** Detecting the number of clusters of individuals using the software STRUCTURE: a simulation study. *Molecular Ecology* **14**:2611–2620 DOI [10.1111/j.1365-294X.2005.02553.x](https://doi.org/10.1111/j.1365-294X.2005.02553.x).
- Excoffier L, Laval G, Schneider S. 2005.** Arlequin (version 3.0): an integrated software package for population genetics data analysis. *Evolutionary Bioinformatics* **1**:47–50.
- Fu YX. 1997.** Statistical tests of neutrality of mutations against population growth, hitchhiking and background selection. *Genetics* **147**:915–925.
- Funk DJ, Omland KE. 2003.** Species-level paraphyly and polyphyly: frequency, causes, and consequences, with insights from animal mitochondrial DNA. *Annual Review of Ecology, Evolution, and Systematics* **34**:397–423
DOI [10.1146/annurev.ecolsys.34.011802.132421](https://doi.org/10.1146/annurev.ecolsys.34.011802.132421).
- Glaubitz JC. 2004.** Convert: a user-friendly program to reformat diploid genotypic data for commonly used population genetic software packages. *Molecular Ecology Notes* **4**:309–310 DOI [10.1111/j.1471-8286.2004.00597.x](https://doi.org/10.1111/j.1471-8286.2004.00597.x).
- Grandin U. 2006.** PC-ORD version 5: a user-friendly toolbox for ecologists. *Journal of Vegetation Science* **17**:843–844 DOI [10.1111/j.1654-1103.2006.tb02508.x](https://doi.org/10.1111/j.1654-1103.2006.tb02508.x).
- Guo WX, Xia ZQ. 2007.** Study on ecological flow in the middle and lower reaches of the Yangtze River. *Journal of Hydraulic Engineering* **10**:618–623.
- Holland MM, Parson W. 2011.** GeneMarker[®] HID: a reliable software tool for the analysis of forensic STR data. *Journal of Forensic Sciences* **56**:29–35
DOI [10.1111/j.1556-4029.2010.01565.x](https://doi.org/10.1111/j.1556-4029.2010.01565.x).
- Hubisz MJ, Falush D, Stephens M, Pritchard JK. 2009.** Inferring weak population structure with the assistance of sample group information. *Molecular Ecology Resources* **9**:1322–1332 DOI [10.1111/j.1755-0998.2009.02591.x](https://doi.org/10.1111/j.1755-0998.2009.02591.x).
- Katoh K, Rozewicki J, Yamada KD. 2019.** MAFFT online service: multiple sequence alignment, interactive sequence choice and visualization. *Briefings in Bioinformatics* **20**:1160–1166.
- Lei L, Feng L, Jian TR, Yue GH. 2012.** Characterization and multiplex genotyping of novel microsatellites from Asian swamp eel, *Monopterus albus*. *Conservation Genetics Resources* **4**:363–365 DOI [10.1007/s12686-011-9549-6](https://doi.org/10.1007/s12686-011-9549-6).

- Li W, Liao X, Yu X, Cheng L, Tong J. 2007.** Isolation and characterization of polymorphic microsatellites in a sex-reversal fish, rice field eel (*Monopterus albus*). *Molecular Ecology Notes* 7:705–707 DOI [10.1111/j.1471-8286.2007.01683.x](https://doi.org/10.1111/j.1471-8286.2007.01683.x).
- Li W, Sun WX, Fan J, Zhang CC. 2013.** Genetic diversity of wild and cultured swamp eel (*Monopterus albus*) populations from central China revealed by ISSR markers. *Biologia* 68:727–732.
- Liang H, Guo S, Li Z, Luo X, Zou G. 2016.** Assessment of genetic diversity and population structure of swamp eel *Monopterus albus* in China. *Biochemical Systematics and Ecology* 68:81–87 DOI [10.1016/j.bse.2016.06.006](https://doi.org/10.1016/j.bse.2016.06.006).
- Liem KF. 1963.** Sex reversal as a natural process in the synbranchiform fish *Monopterus albus*. *Copeia* 2:303–312.
- Liu CK. 1944.** Rudimentary hermaphroditism in the symbranchoid eel, *Monopterus favanensis*. *Sinensia* 15:1–18.
- Mazzoni T, Nostro FLo, Antoneli F, Quagio-Grassiotto I. 2018.** Action of the Metalloproteinases in Gonadal Remodeling during Sex Reversal in the Sequential Hermaphroditism of the Teleostei Fish *Synbranchus marmoratus* (Synbranchiformes: Synbranchidae). *Cell* 7:34 DOI [10.3390/cells7050034](https://doi.org/10.3390/cells7050034).
- Nelson JS, Grande TC, Wilson MV. 2016.** *Fishes of the world*. Hoboken: John Wiley & Sons Press.
- Qu XC. 2018.** Sex determination and control in eels. In: *Sex control in aquaculture*. Chichester: John Wiley & Sons Press, 775–792.
- Qu Y, Zhang R, Quan Q, Song G, Li SH, Lei F. 2012.** Incomplete lineage sorting or secondary admixture: disentangling historical divergence from recent gene flow in the Vinous-throated parrotbill (*Paradoxornis webbianus*). *Molecular Ecology* 21:6117–6133 DOI [10.1111/mec.12080](https://doi.org/10.1111/mec.12080).
- Rogers AR, Harpending H. 1992.** Population growth makes waves in the distribution of pairwise genetic differences. *Molecular Biology and Evolution* 9:552–569.
- Rozas J, Ferrer-Mata A, Sánchez-DelBarrio JC, Guirao-Rico S, Librado P, Ramos-Onsins SE, Sánchez-Gracia A. 2017.** DnaSP 6: DNA sequence polymorphism analysis of large data sets. *Molecular Biology and Evolution* 34:3299–3302 DOI [10.1093/molbev/msx248](https://doi.org/10.1093/molbev/msx248).
- Saccone C, De Giorgi C, Gissi C, Pesole G, Reyes A. 1999.** Evolutionary genomics in Metazoa: the mitochondrial DNA as a model system. *Gene* 238:195–209 DOI [10.1016/S0378-1119\(99\)00270-X](https://doi.org/10.1016/S0378-1119(99)00270-X).
- Sambrook J, Fritsch EF, Maniatis T. 1989.** *Molecular cloning: a laboratory manual*. New York: Cold spring harbor laboratory press.
- Slatkin M, Barton NH. 1989.** A comparison of three indirect methods for estimating average levels of gene flow. *Evolution* 43:1349–1368 DOI [10.1111/j.1558-5646.1989.tb02587.x](https://doi.org/10.1111/j.1558-5646.1989.tb02587.x).
- Suchard MA, Lemey P, Baele G, Ayres DL, Drummond AJ, Rambaut A. 2018.** Bayesian phylogenetic and phylodynamic data integration using BEAST 1.10. *Virus Evolution* 4:vey016.

- Tajima F. 1989.** Statistical method for testing the neutral mutation hypothesis by DNA polymorphism. *Genetics* **123**:585–595.
- Yang JQ, Hsu KC, Liu ZZ, Su LW, Kuo PH, Tang WQ, Zhou ZC, Liu D, Bao BL, Lin HD. 2016.** The population history of *Garra orientalis* (Teleostei: Cyprinidae) using mitochondrial DNA and microsatellite data with approximate Bayesian computation. *BMC Evolutionary Biology* **16**:73 DOI [10.1186/s12862-016-0645-9](https://doi.org/10.1186/s12862-016-0645-9).
- Yeh FC, Yang RC, Boyle TB, Ye ZH, Mao JX. 1997.** POPGENE, the user-friendly shareware for population genetic analysis. *Molecular Biology and Biotechnology Centre, University of Alberta, Canada* **10**:295–301.
- Zarza E, Reynoso VH, Emerson BC. 2011.** Discordant patterns of geographic variation between mitochondrial and microsatellite markers in the Mexican black iguana (*Ctenosaura pectinata*) in a contact zone. *Journal of Biogeography* **38**:1394–1405 DOI [10.1111/j.1365-2699.2011.02485.x](https://doi.org/10.1111/j.1365-2699.2011.02485.x).
- Zhang W, YT LI, Jiang L. 2008.** Fluvial process change of the typical multi-branched meandering reach in the mid-down Yangtze River after three gorges dam impoundment. *Journal of Sichuan University (Engineering Science Edition)* **40**:17–24.
- Zhuo Y, Hu H, Zhang L, Shu M. 2011.** Microsatellite analysis of genetic diversity of *Monopterus albus* along the middle and lower reaches of Yangtze River basin. *Biotechnology Bulletin* **11**:187–192.